Numerical Analysis of Phase Change Material with Variable Heat Load using OpenFOAM

Syed Aaqib Ahmed A[1#], Nikhil Chitnavis[2], Chandan Bose[3], Divyesh Variya[4],

[1]Sr. Design Engineer, TTCADD, Vellore, India
[2]Indian Institute of Technology Madras, India
[3]Aerospace Engineering, University of Birmingham, UK
[4]Ecozen Solutions Pvt. Ltd., Pune, Maharastra, India
[*]Email: syedaaqibahmeda@gmail.com

Abstract

This study aims to conduct numerical investigation of the melting of gallium and ice in a 2D channel using OpenFOAM v1906's `buoyantPimpleFoam` solver with the `solidificationMeltingSource` term. Two mesh sizes of 1800 cells, 7200 cells and 28800 cells are employed to examine mesh sensitivity. The temperature profiles and liquid-phase velocity fields are analysed to characterize the phase change dynamics. The simulation captures melting front progression, convective heat transfer effects, and recirculation patterns in the molten phase, with validation supported by established gallium phase-change studies using enthalpy-porosity method demonstrating the influence of mesh resolution on predicting interface motion and thermal transport during melting.

Keywords: *Phase Change Material, ice, gallium, OpenFOAM*

1. Introduction

Numerous numerical techniques exist for solving moving boundary problems in phase change systems. These techniques focus on conduction-dominated processes. However, recent investigations address convection effects during freezing in thermal cavities using temperature formulations with deforming grids. Alternatively, enthalpy formulations enable fixed-grid solutions by eliminating explicit interface tracking, as demonstrated by Morgan (1981), Gartling (1978), and Voller et al. (1987), simplifying numerical modeling for complex systems.

Fixed-grid methods face challenges in enforcing zero velocity in solidifying regions. Morgan (1981) sets velocities to zero when latent heat content reaches a threshold, while Gartling (1978) links viscosity to latent heat to mimic phase change (Brent et al. 1988; Wolff & Viskanta 1988). Voller et al. (1987) treat phase-changing cells as porous media, using a Darcy source term

to suppress velocities as solidification completes, offering a robust approach for natural convection problems.

2. Problem Statement

Precise numerical modeling of melting processes for phase-change materials remains challenging due to the complex interaction between heat transfer and fluid flow dynamics. The parameters like melting front progression, temperature distribution, and convective recirculation patterns in a 2D channel with lateral isothermal walls needs further investigation. In particular, the effect of mesh size on the characteristics of the phase change.

2.1 Objectives and scope of present work

To simulate the melting of Ice, using `buoyantPimpleFoam` (transient state) solver.

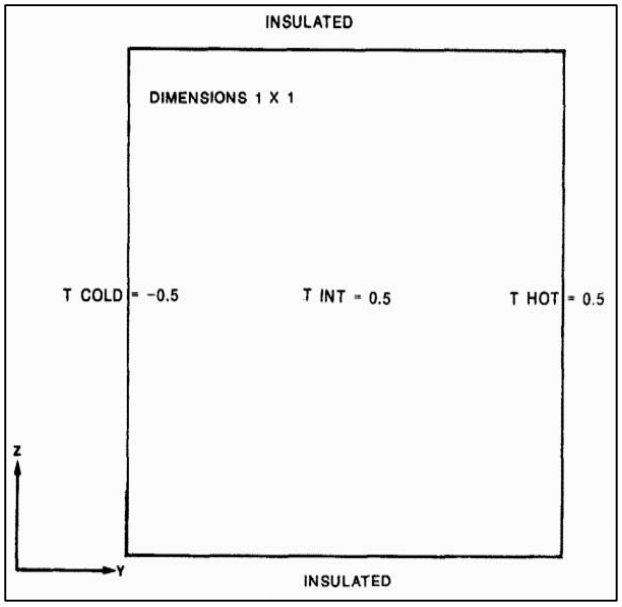

Fig. 1 Schematic flow domain (adapted from Voller and Prakash 1987)

Accordingly, in the OpenFOAM, `SolidificationMelting` Source (adds the source term to the Momentum & Energy Equation) using fVOption.

Enthalpy – Porosity Method

Following are the assumptions:

1. Incompressible, laminar and Newtonian flow in the liquid phase.
2. Constant physical properties of liquid and solid phase.
3. Boussinesq approximation for density variation of liquid phase with temperature.
4. Solid phase is considered as non-deforming (that is., NO internal stresses).

In the literature, employing these methods there are investigations on the phase-change characteristics (Vignesh 2021; Singh et al. 2019; Mahdi 2019)

3. Governing Equations

For the numerical simulation, the conservation equations of mass and momentum are applied. Accordingly, the continuity equation is given as:

$$\frac{\partial v}{\partial y} + \frac{\partial w}{\partial z} = 0 \quad (1)$$

where v and w are velocities in y and z direction respectively.

$$\frac{\partial(\rho w)}{\partial t} + \text{div}\,(\rho \text{uw}) = div(\mu\ grad\ w) - \frac{\partial P}{\partial z} + S_d + S_b \quad (2)$$

where P is pressure, ρ is density, μ is the viscosity of melt, u = (v, w), and S_d and S_b are the source terms and are defined below.

The source term S_d is used to modify the momentum equations in the mushy region. $S_d = -Av$. S_d is expected to dominate all other terms in momentum equation, resulting in v=0. For further details, Voller & Prakash (1987) may be referred.

$$A = -\frac{C(1-\lambda)^2}{(\lambda^3+q)} \quad (3)$$

Where C depends on the porous media morphology (1.6×10^3), q is a constant (0.001) and λ is the porosity.

The Buoyancy (gravity) source term S_b is, for the Boussinesq treatment to be valid, given as:

$$S_b = \rho g \beta (T - T_{ref}) \quad (4)$$

where β is the thermal expansion coefficient and subscript ref is the reference value of the sensible heat.

Energy equation:

$$\frac{\partial(\rho h)}{\partial t} + \text{div}\,(\rho \text{uh}) = div(\mu\ grad\ h) - S_h \quad (5)$$

where α is the thermal diffusivity, S_h is phase related source term (Voller et al. 1987).

$$S_h = \frac{\partial(\rho \Delta H)}{\partial t} + \text{div}\,(\rho \text{u} \Delta \text{H}) \quad (6)$$

The enthalpy of the material H = cT+ΔH, where cT is the sensible heat and the ΔH is the latent heat. Relation to transform $g_l = 1$ into $g_l = 0$ as temperatures become lower than the melting temperature i.e., $T < T_f$. Discretizing the energy equation explicitly, and taking the temperature derivative of both sides

$$\frac{\partial g_l}{\partial T} = -\frac{C_P}{L_f} \quad (7)$$

$$g_l^{n+1} = g_l^n + \frac{\gamma C_P}{L_f}\left(T - T_f\right) \quad (8)$$

$$g_l^{n+1} = max[0, min(1, g_l^{n+1})] \quad (9)$$

The superscripts n+1 and n refer to the present and last iteration levels respectively, and γ is an under-relaxation factor (of order 1).

4. Creation of Mesh and Simulation

4.1 Geometry and Mesh

The geometry considered for the present investigation is 2D (rectangular section) of 6mm x 12mm. Since the geometry is simple, the geometry was created using the blockMesh utility of OpenFOAM. This utility employs a dictionary file referred as `blockMeshDict` and this dictionary file is generally placed in the constant/polyMesh directory. Also, the mesh is generated and stored in the same directory as points, faces, internal faces and cells files. Three blocks are considered. The grading of the mesh is done using simple-grading, and there was no refinement of the mesh carried out (refer Fig. 4.1 and Appendix). Accordingly, the mesh constitutes around 7200 and 1800 cells and shown in Fig. 4.2.

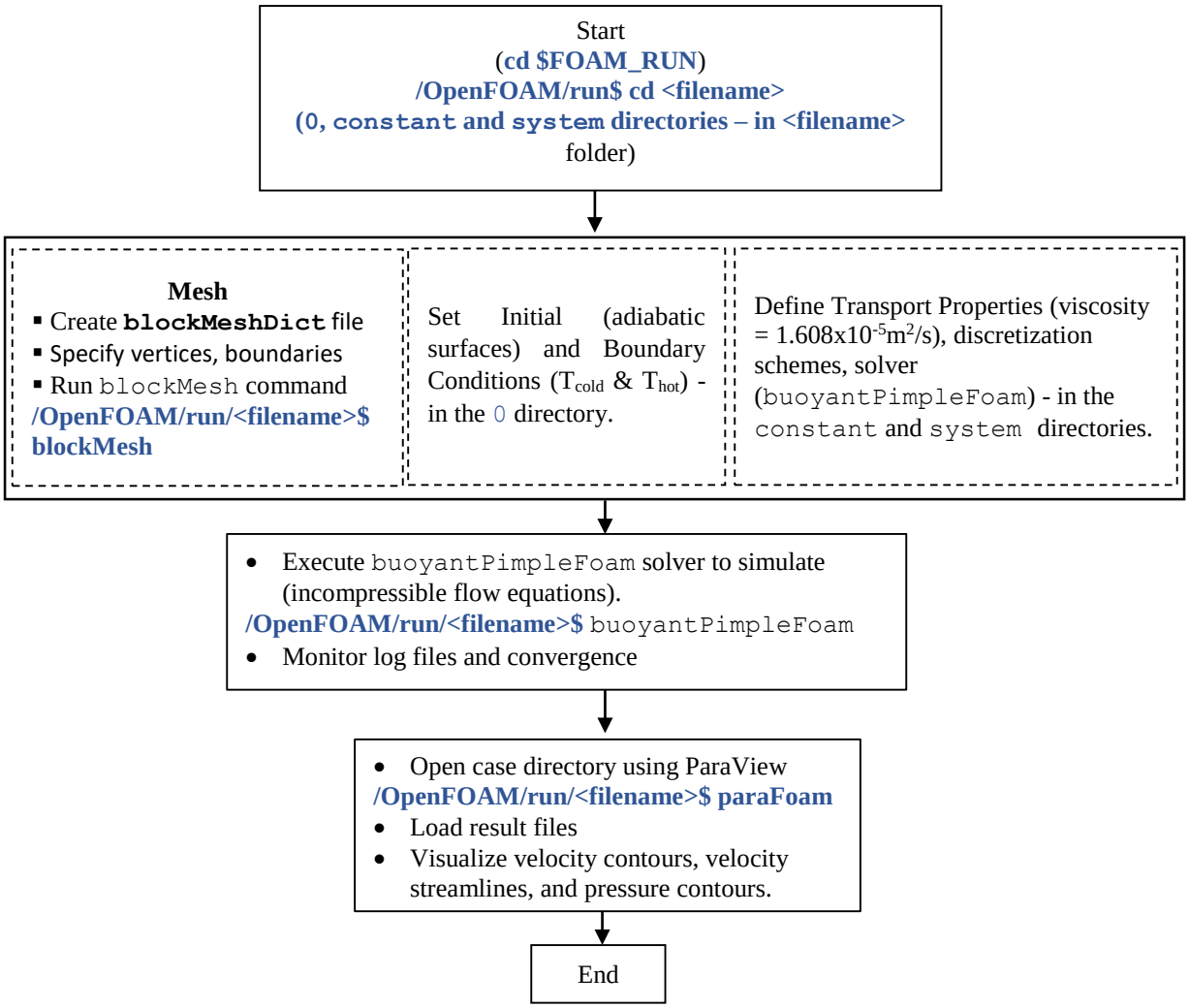

Fig. 4.1 Procedure to simulate using `OpenFOAM`

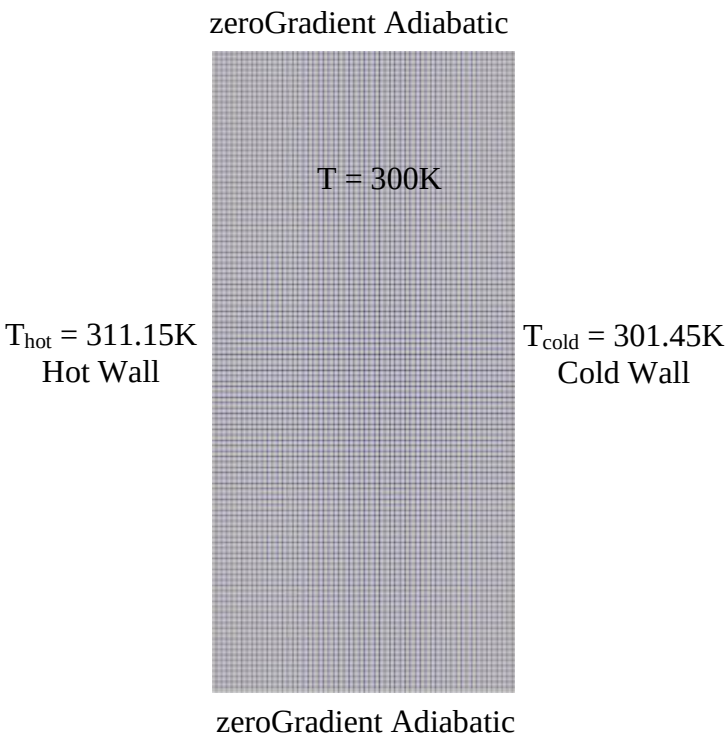

Fig. 4.2 Generated mesh (L = 6mm x H = 12mm)

4.2 Initial and Boundary Conditions

In the present analysis, the initial temperature is set as 300K. The two surfaces (top and bottom) are considered adiabatic. The other two surfaces (left and right) are set as T_{hot} = 311.45K and T_{cold} = 301.45K respectively. For the analysis of effect mesh size, the boundary temperatures are set as T_{hot} = 283.15K and T_{cold} = 273.12K. Accordingly, the boundary conditions are indicated as field files such as T in time directories.

Table 4.1 Details of Boundary conditions

Description	T
Top & Bottom wall	zeroGradient
Right & Left wall	T_{cold} = 301.45K & 273.15K and T_{hot} = 311.15K & 283.15K
frontAndBack	empty

4.3 Solver

In the present analysis, `buoyantPimpleFoam` solver is employed. The `buoyantPimpleFoam` is a transient solver for turbulent flows driven by buoyancy effects from temperature-induced density differences. It employs the PIMPLE algorithm to solve momentum and pressure equations, and suitable for transient heat transfer simulations. Further, the solver considers the energy equation to model temperature distribution and heat transfer. Typically, in the analysis of applications like ventilation, electronic cooling, solar collectors, and nuclear reactor analysis, this `buoyantPimpleFoam` solver is generally employed.

5. Results and Discussions

5.1 Simulated results

In the present work, there are two sets of simulations conducted. For the first set of simulations, the mesh of 7200 cells are fixed. With this mesh size of 7200 cells, the melting characteristics like the liquid-solid interface propagation, the temperature and velocity distribution for ice and gallium are evaluated. The simulations are carried out for a time period of 700sec. Accordingly, these parameters for the ice are described below for different time periods from 30sec to 700 sec

in Fig. 5.1 – Fig. 5.4, and the melting characteristics for gallium are given below in Fig 5.5 to Fig. 5.8 respectively.

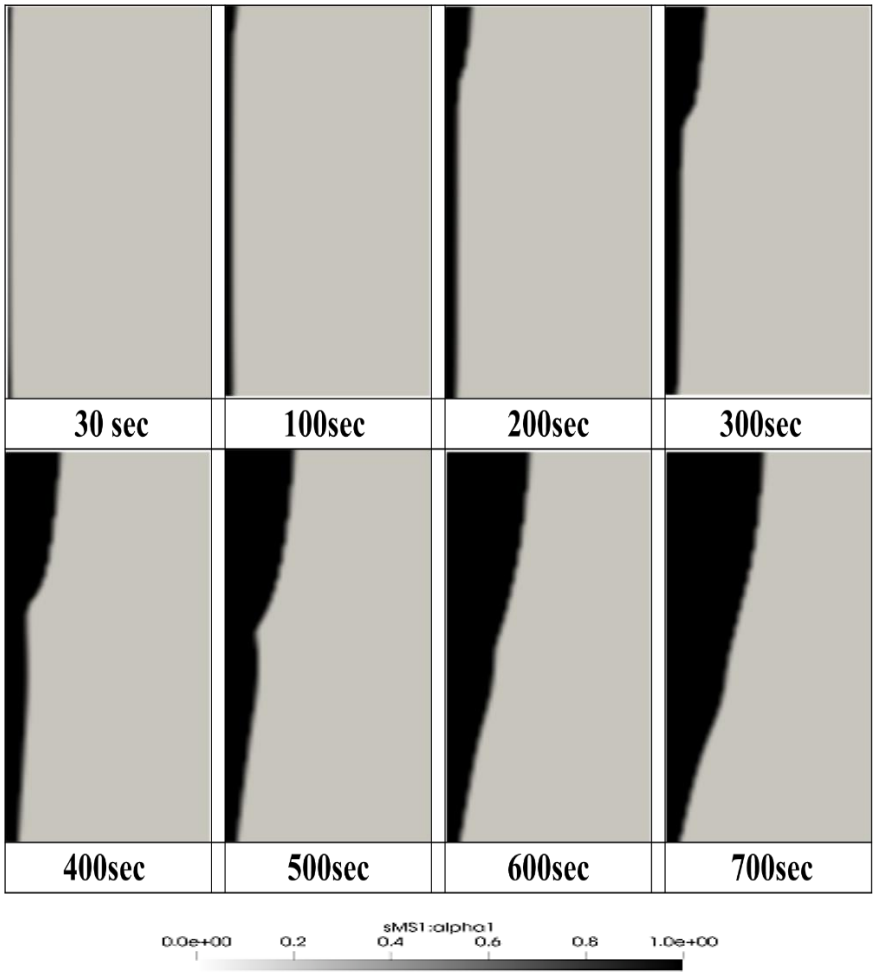

Fig. 5.1 Volume fraction of water (liquid) and ice (solid) at different time periods.

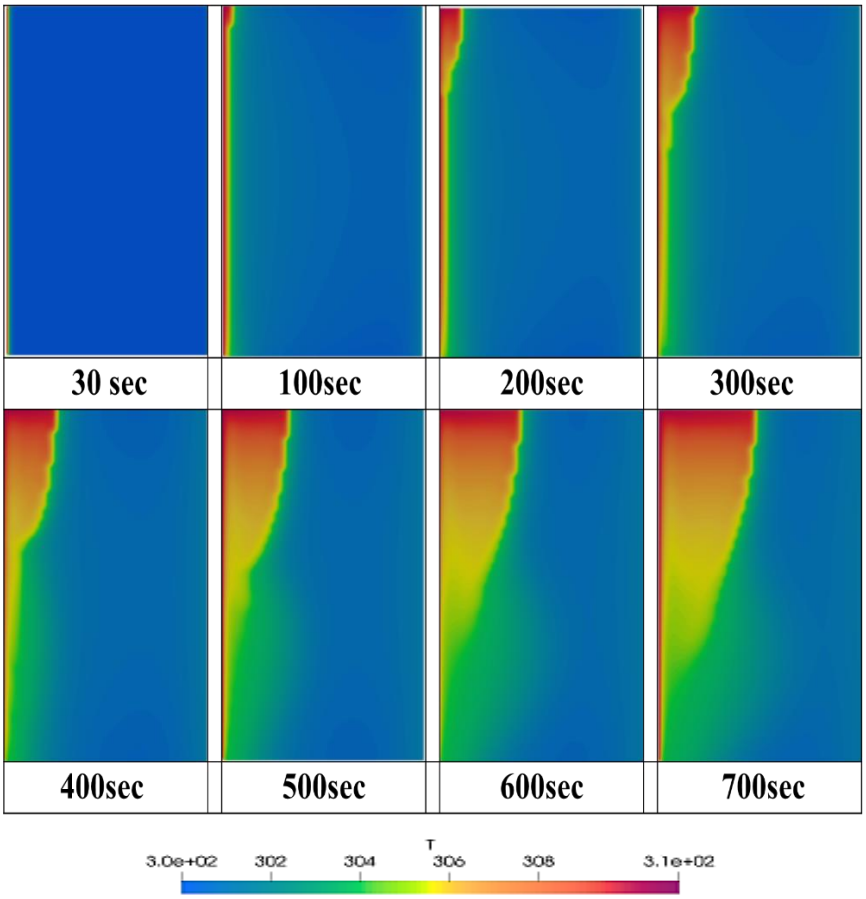

Fig. 5.2 Temperature distribution of water (liquid) and ice (solid) at different time periods.

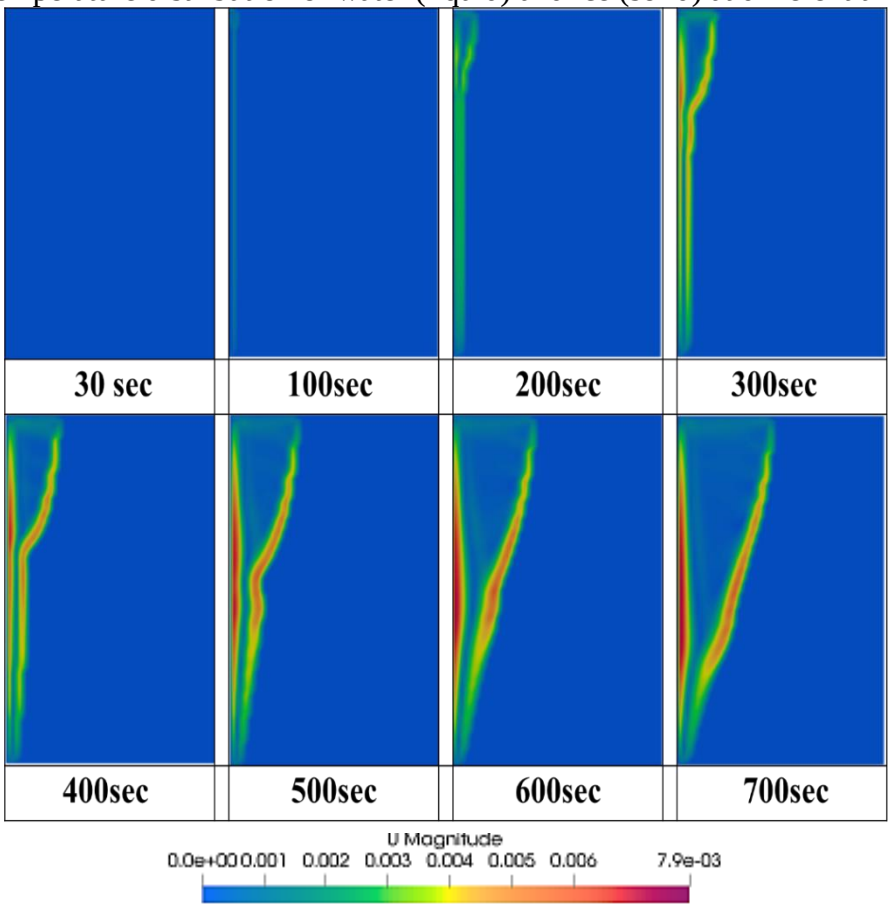

Fig. 5.3 Velocity distribution of water (liquid) and ice (solid) at different time periods.

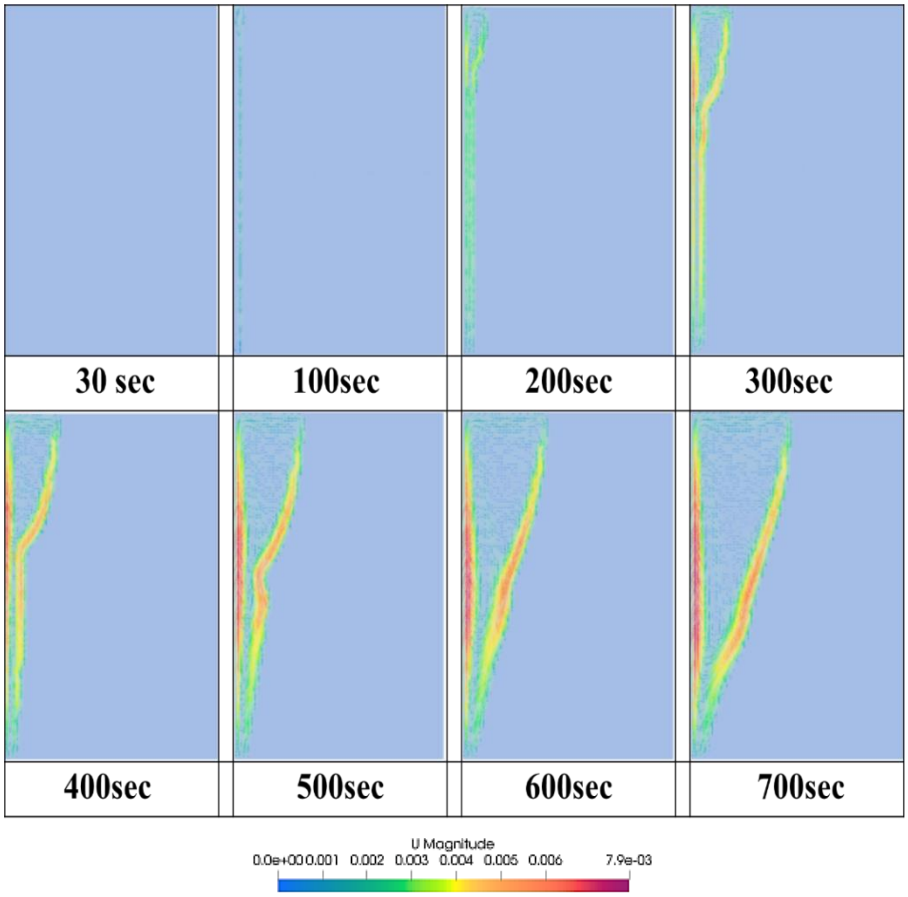

Fig. 5.4 Velocity Contours of water (liquid) and ice (solid) at different time periods.

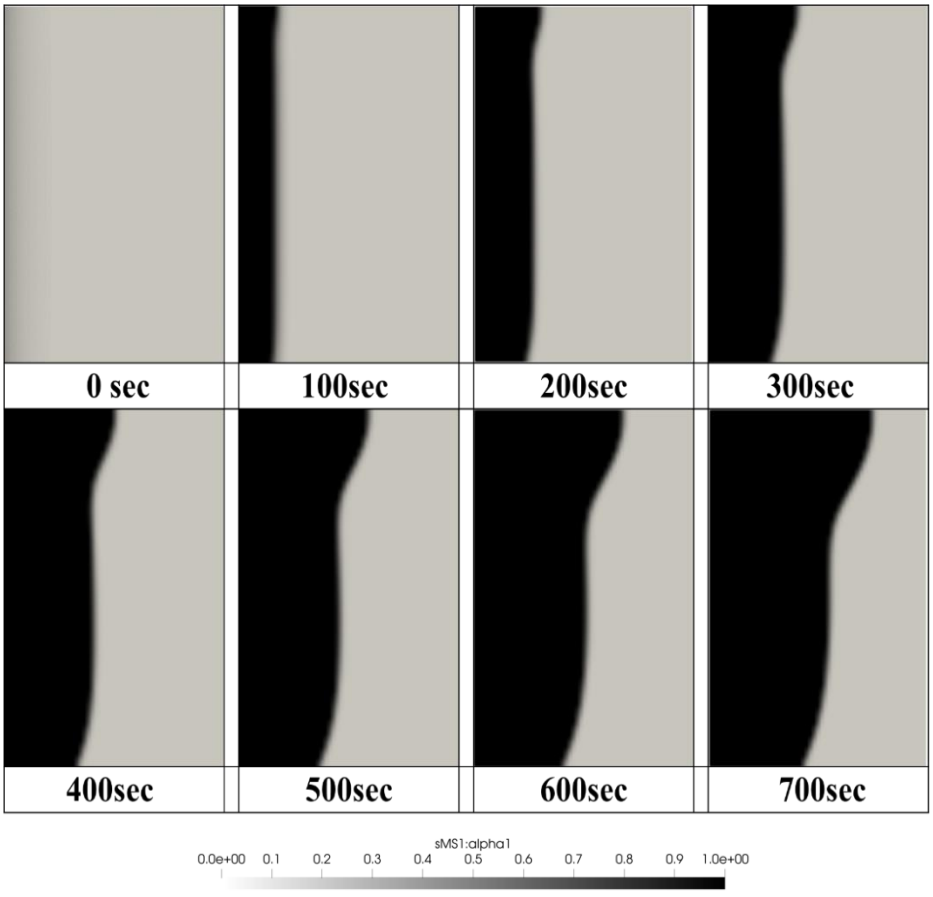

Fig. 5.5 Volume fraction of liquid phase and solid phase of Gallium at different time periods.

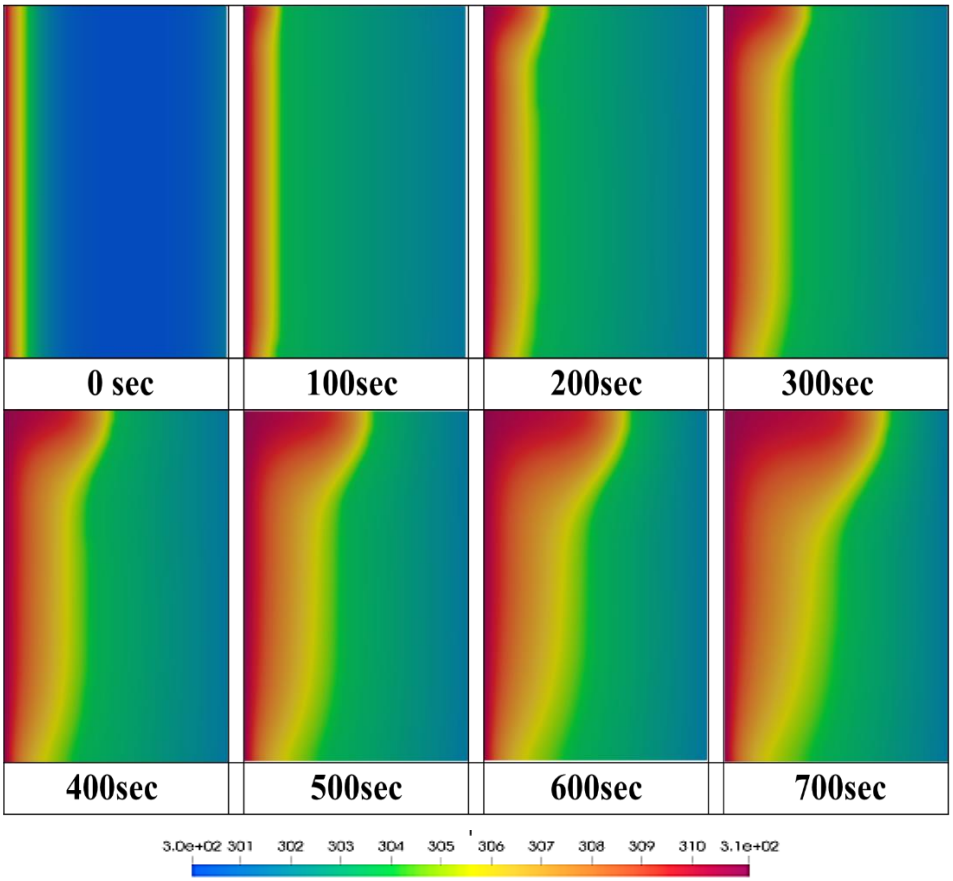

Fig. 5.6 Temperature distribution of liquid phase and solid phase of Gallium at different time periods.

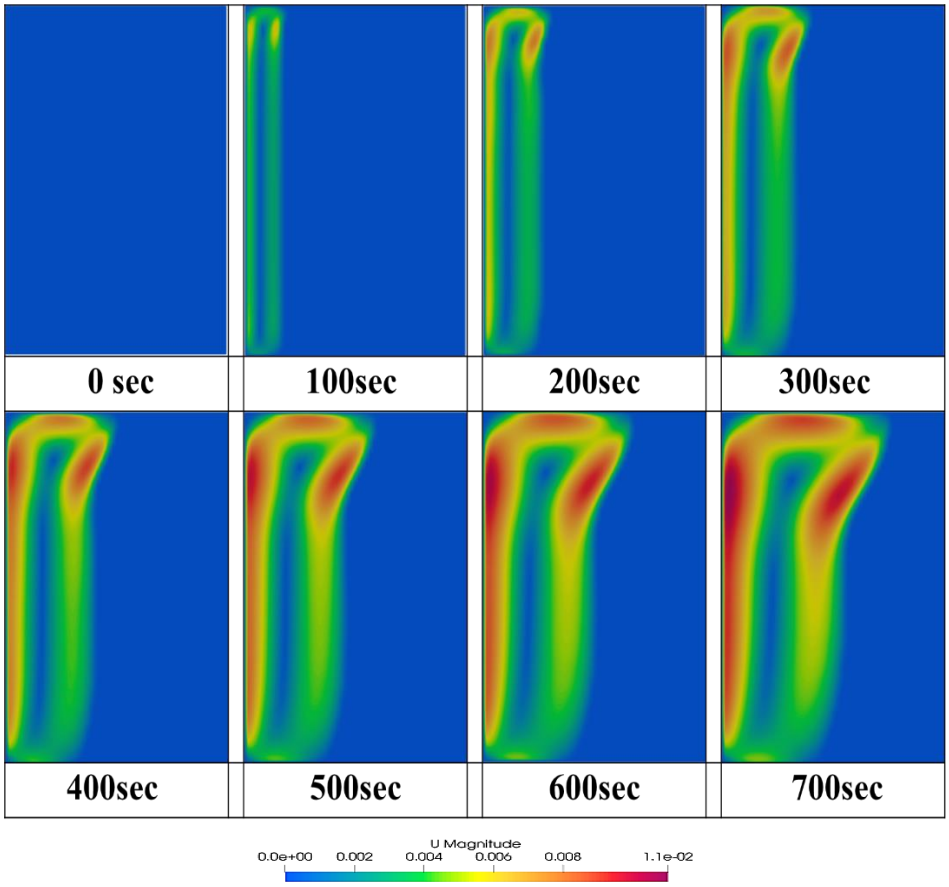

Fig. 5.7 Velocity distribution of liquid phase and solid phase of Gallium at different time periods.

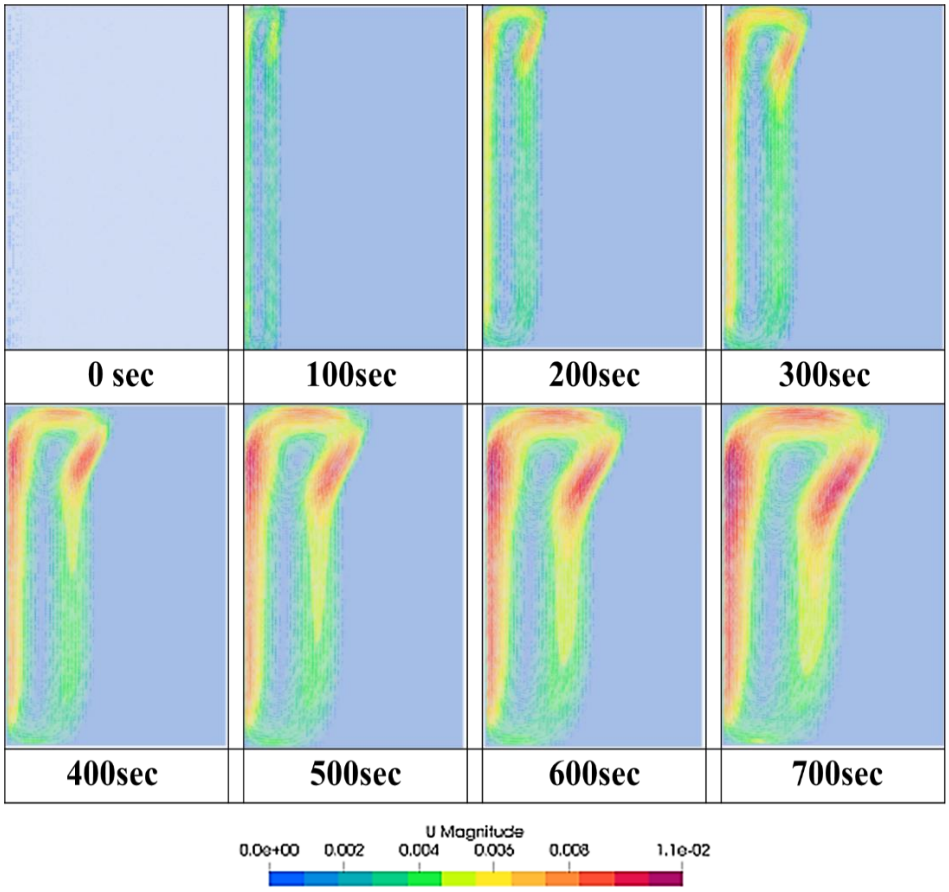

Fig. 5.8 Velocity Contours of liquid phase and solid phase of Gallium at different time periods.

From the above figures, it may be noted that, for both ice and gallium, the characteristics remain very much similar. However, the characteristics for gallium are found to be enhanced compared to that of the ice. For instance, the liquid-solid interface propagation is wide for gallium compared to the ice. Similarly, other parameters like temperature distribution and velocity of liquid phase are higher for gallium than that of the ice.

5.2 Effect of Mesh size

Further, to study the effect of mesh size on the same melting parameters of liquid-solid interface propagation, temperature and velocity profile, simulations are carried out for three mesh sizes of 28800, 7200 and 1800 cells. In this set of simulations, only ice is considered. The results of these simulations are shown below in Fig. 5.9. From the figure, it is evident that the mesh size affects the parameters like volume fraction, temperature and velocity characteristics. In particular, the liquid volume fraction and temperature at the liquid-solid interface are higher than that observed with mesh size of 1800. However, the liquid phase velocity with mesh size of 7200 cells is slightly lower than with mesh size of 1800 cells. Further, the contours of these parameters like

volume fraction, temperature and velocity characteristics are shown in Fig 5.10 – Fig. 5.13 respectively.

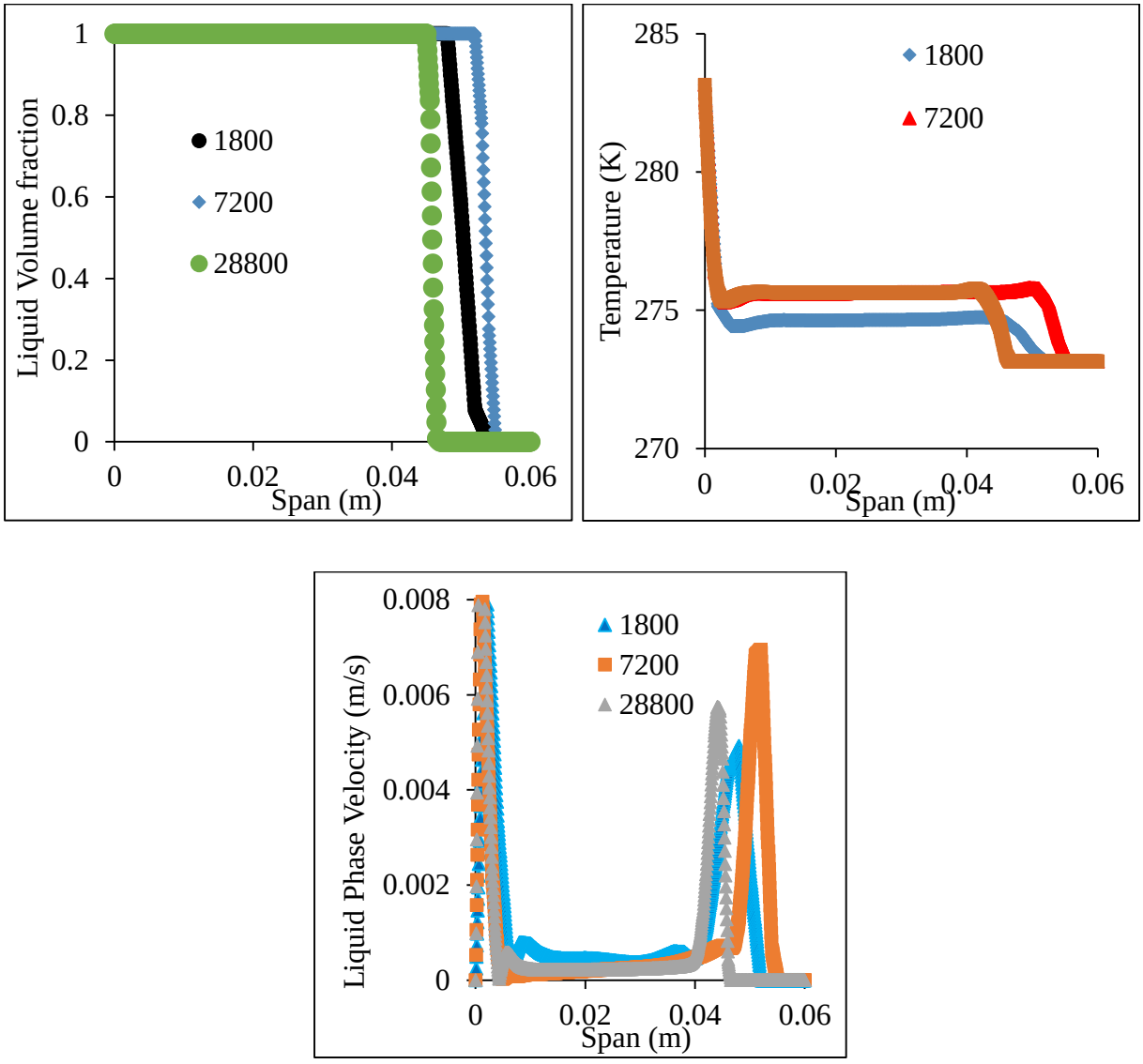

Fig. 5.9(a) – (c) Effect of mesh size.

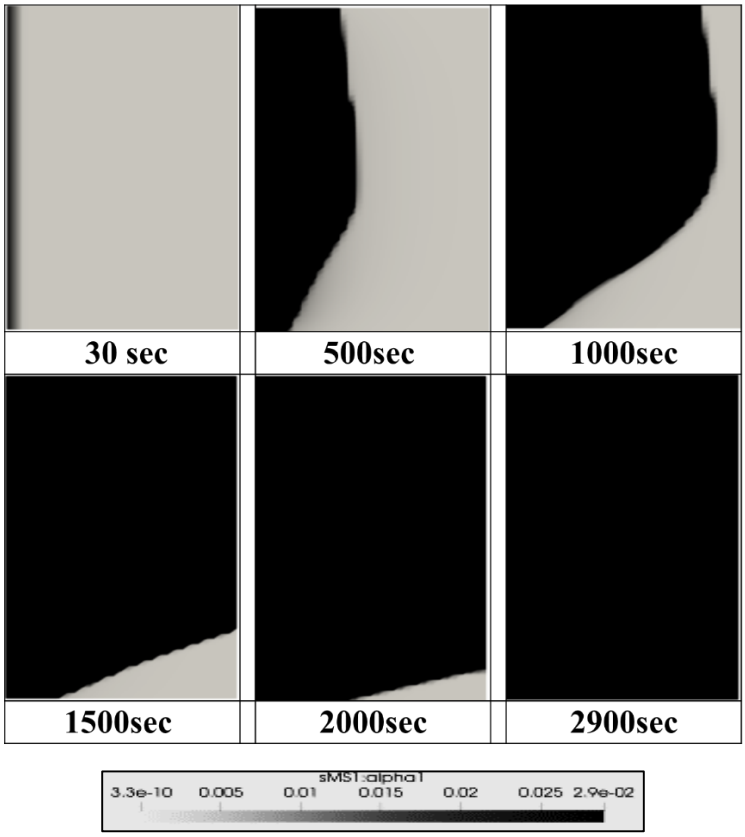

Fig. 5.10 Volume fraction of liquid phase (water) and solid phase (ice) at different time periods.

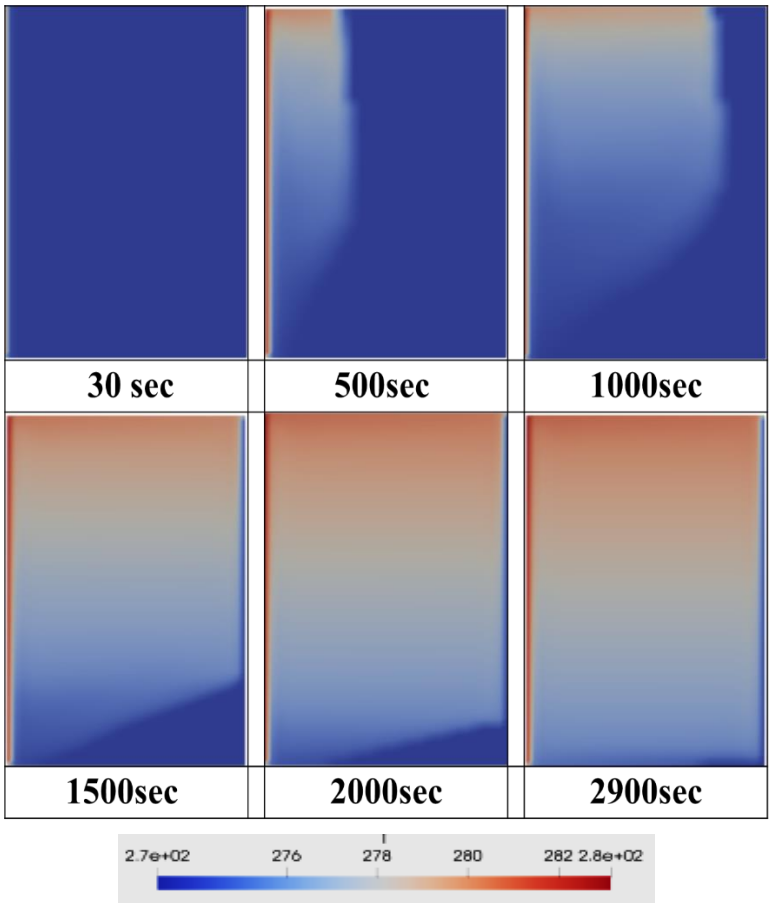

Fig. 5.11 Temperature distribution across liquid-solid (water - ice) interface at different time periods.

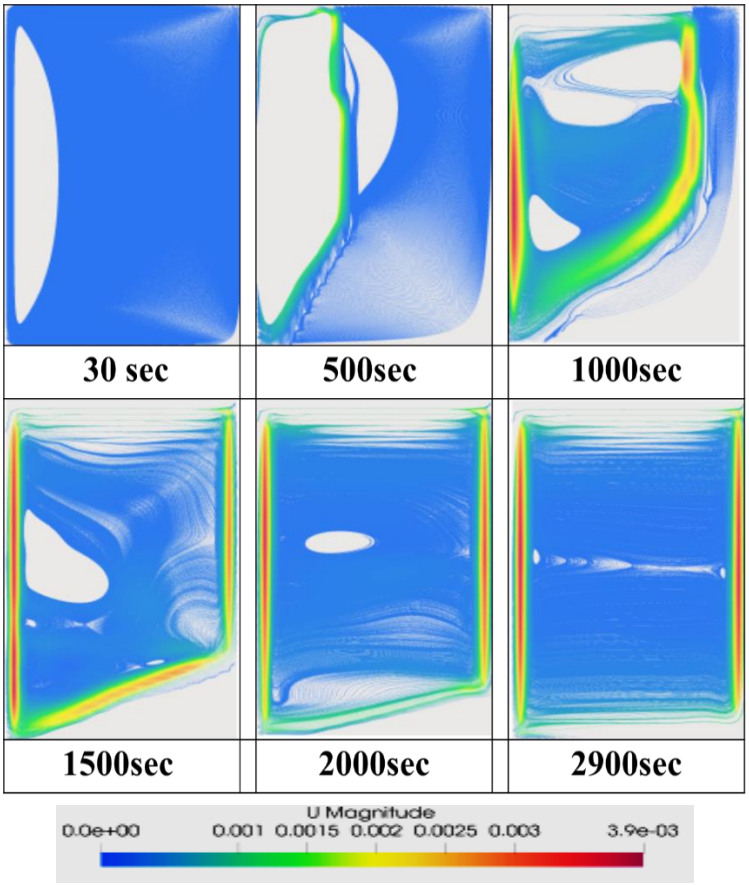

Fig. 5.12 Temperature distribution across liquid-solid (water - ice) interface at different time periods.

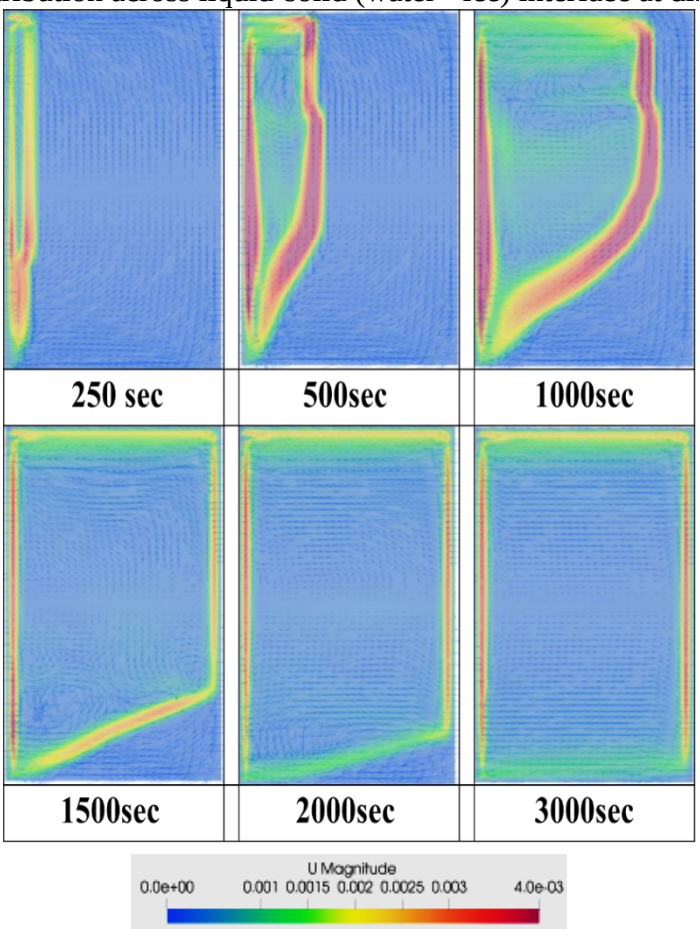

Fig. 5.13 Velocity streamlines across liquid-solid (water - ice) interface at different time periods.

5.3 Discussion

This numerical study investigates the melting dynamics of gallium and ice within a two-dimensional channel featuring isothermal boundary conditions, employing OpenFOAM v1906's `buoyantPimpleFoam` solver coupled with the `solidificationMeltingSource` term to accurately capture the phase transition phenomena. The computational analysis utilizes two distinct mesh resolutions - a coarser grid of 1800 cells and a refined configuration of 28800 cells - to systematically evaluate mesh dependency effects on solution accuracy, particularly focusing on the prediction of interface motion and heat transfer characteristics. The investigation examines detailed temperature distributions and liquid-phase velocity fields, revealing critical insights into melting front propagation, convective heat transfer mechanisms, and the development of characteristic recirculation patterns within the molten phase. The study further highlights the importance of mesh size in characterising the interaction between conduction-dominated and convection-dominated regimes, thus offering significant comprehension on the phase-change phenomenon.

6. Conclusions

Employing OpenFOAM's `buoyantPimpleFoam` solver with the `solidificationMeltingSource` term, the present study effectively characterized the Phase Change dynamics of gallium and ice.

- Temperature distributions and velocity fields specify different melting stages, including conduction-dominated initial stages and convection-dominated stages.
- There is considerable enhancement of heat transfer due to recirculation patterns in the molten phase, thus affecting the melting process.
- The mesh size critically effects the precision of interface tracking, particularly in convection-dominated regimes.
- The smaller mesh size of 28800 cells enhances solid-liquid interface of melting front, its propagation and thus improving the heat transfer compared to a coarser grid of 1800 cells.

References

1. Singh,A., Kumar, A., & Kumar, A., (2019). Numerical Modelling of Pure Metal Solidification using OpenFOAM. 2019. ffhal-02101324v2
2. Wolff, F., & Viskanta, R., (1988). Solidification of a pure metal at a vertical wall in the presence of liquid superheat, International journal of heat and mass transfer, vol. 31(8), pp 1735-1744.

3. Jun, N., & Beckermann, C., (1991). A volume-averaged two-phase model for transport phenomena during solidification, Metallurgical Transactions B, vol 22(3), pp 349
4. Brent, A.D., Voller, V.R., Reid, K.T.J., (1988). Enthalpy-porosity technique for modelling convection-diffusion phase change: application to the melting of a pure metal, Numerical Heat Transfer, Part A Applications, vol 13(3), pp 297-318.
5. Mahdi, T. R., (2019). solidificationMeltingSource: A Built-in fvOption in OpenFOAM for Simulating Isothermal Solidification: Selected Papers of the 11th Workshop, RWTH Aachen University, January 2019 DOI: 10.1007/978-3-319-60846-4_32
6. Morgan, K., (1981). A numerical analysis of freezing and melting with convection, computer methods in applied mechanics and engineering, 28, 275-284, North-Holland Publishing Company
7. Gartling, D.K., (1978), Finite element analysis of convective heat transfer problems with change of phase, in: K. Morgan, C. Taylor and C.A. Brebbia, eds., Computer Methods in Fluids (Pentech, London, 1980).
8. José, H. N. E, De Césaro, R.O, Alberto, L.O.R, Biserni,C., & Garai,M., (2019). Fixed Grid Numerical Models for Solidification and Melting of Phase Change Materials (PCMs), Appl. Sci. 2019, 9, 4334; doi:10.3390/app9204334
9. Hu, H., & Argyropoulos, S.A., (1996). Mathematical modelling of solidification and melting: A review. Model. Simul. Mater. Sci. Eng. 4, 371–396
10. Voller, V.R., Cross, M., & Markatos, N.C., (1987). An enthalpy method for convection/diffusion phase change. Int. J. Numer. Methods Eng. 24, 271–284.
11. Voller, V.R., Cross, M., & Markatos, N.C., (1987). An enthalpy method for convection/diffusion phase changes. Inr. J. Num. Meth. Engg 24,271-284.
12. Vignesh. S.P, (2021). Numerical Simulation Melting of Ice using OpenFOAM, Anna University, Chennai
13. Brinkman,H.C., (1947). A calculation of the viscous force exerted by a flowing fluid on a dense swarm of particles, Appl. Scient. Res., 27-34.

Appendix

```
/*--------------------------------*- C++ -*----------------------------------*\
| =========                 |                                                 |
| \\      /  F ield         | OpenFOAM: The Open Source CFD Toolbox           |
|  \\    /   O peration     | Version:  3.0.0                                 |
|   \\  /    A nd           | Web:      www.OpenFOAM.org                      |
|    \\/     M anipulation  |                                                 |
\*---------------------------------------------------------------------------*/
FoamFile
{
    version     2.0;
    format      ascii;
    class       dictionary;
    location    "constant";
    object      thermophysicalProperties;
}
```

```
// * * * * * * * * * * * * * * * * * * * * * * * * * * * * * * * * * * * * * * * * * * * * //

thermoType
{
    type         heRhoThermo;   // general thermophysical model based on enthalpy, and density.
    mixture      pureMixture;   // General thermophysical model calucaltion for gas mixtures.
    transport    const;
    thermo       hConst;        // Constant specific heat with evaluation of enthalpy and entropy.
    equationOfState perfectFluid; // Perfect gas equation of state.
    specie       specie;
    energy       sensibleInternalEnergy;
}

mixture
{
    specie
    {
        nMoles      1;      // number of moles of component.
        molWeight   18;     // grams per mole of specie.
    }
    equationOfState
    {
        R           3000;   // fluid constant
        rho0        999.8;  // reference density
    }
    thermodynamics
    {
        Cp          4210;   // specific heat capacity
        Hf          0;      // enthalpy change (heat absorbed or released)
    }
    transport
    {
        mu          1.3e-3; // dynamic viscosity of a fluid
        Pr          9.652;  // Prandtl Number
    }
}

FoamFile
{
    version     2.0;
    format      ascii;
    class       dictionary;
```

```
    location    "constant";
    object      fvOptions;
}
// * * * * * * * * * * * * * * * * * * * * * * * * * * * * * * * * * * * * * * * * * * * * //
sMS1
    {
        type            solidificationMeltingSource; // fvOption type.
        active          yes;

        solidificationMeltingSourceCoeffs
        {
            selectionMode   cellZone;       // cell saturation mode
            cellZone        solid;
            Tsol            273.15;         // Saturation temperature [K]
            L               80160;          // Enthalpy of fusion for water [J/Kg]
            thermoMode      thermo;         // Retrieve thermo properties
            beta            1.2e-4;         // Thermal expansion Coefficient [1/K]
            rhoRef          6093;           // Reference Solid Density [Kg/m^3]
            Cu              1.6e+06;        // Momentum Sink Coefficient
            q               1.0e-03;        // Porosity Coefficient
        }
    }
// * * * * * * * * * * * * * * * * * * * * * * * * * * * * * * * * * * * * * * * * * * * * //
dimensions      [0 0 0 1 0 0 0];

internalField   uniform 273.15;

boundaryField
{
    upperWall
    {
        type            zeroGradient;
    }
    leftWall
    {
        type            fixedValue;
        value           uniform 283.15;
    }
    rightWall
    {
        type            fixedValue;
        value           uniform 273.15;
```

```
    }
    lowerWall
    {
        type            zeroGradient;
    }
    frontAndBack
    {
        type            empty;
    }
}
// * * * * * * * * * * * * * * * * * * * * * * * * * * * * * * * * * * * * * * * * //
FoamFile
{
    version     2.0;
    format      ascii;
    class       dictionary;
    location    "system";
    object      controlDict;
}
// * * * * * * * * * * * * * * * * * * * * * * * * * * * * * * * * * * * * * * * * //

application     buoyantPimpleFoam;   // Solver type used.

startFrom       startTime;

startTime       0;

stopAt          endTime;

endTime         3000;

deltaT          1.0;

writeControl    adjustableRunTime;

writeInterval   2.0;

purgeWrite      0;

writeFormat     ascii;

writePrecision  8;
```

```
writeCompression off;

timeFormat      general;

timePrecision   10;

runTimeModifiable yes;

adjustTimeStep  yes;

maxCo           0.25;

maxDeltaT       1;
maxAlphaCo                                                                  1;//
********************************************************************************* //
\*---------------------------------------------------------------------------*/
FoamFile
{
   version     2.0;
   format      ascii;
   class       dictionary;
   location    "system";
   object      fvSchemes;
}
// * * * * * * * * * * * * * * * * * * * * * * * * * * * * * * * * * * * * * * * * //

ddtSchemes
{
   default         Euler;
}

gradSchemes
{
   default         Gauss linear;
}

divSchemes
{
   default         none;

   // Basic flow equations
```

```
    div(phi,U)      Gauss linearUpwind grad(U);
    div(phi,(p|rho)) Gauss linear;
    div(phi,K)      Gauss linear;  // Newly added for kinetic energy

    // Viscous terms
    div(((rho*nuEff)*dev2(T(grad(U))))) Gauss linear;

    // Turbulence equations (if using k-epsilon)
    div(phi,k)      Gauss upwind;
    div(phi,epsilon) Gauss upwind;

    // Energy equations
    div(phi,h)      Gauss upwind;
    div(phi,e)      Gauss upwind;

    // Optional: For enthalpy-based formulations
    div(phi,T)      Gauss upwind;
}

laplacianSchemes
{
    default         Gauss linear corrected;
}

interpolationSchemes
{
    default         linear;
}

snGradSchemes
{
    default         corrected;
}

\*---------------------------------------------------------------------------*/
FoamFile
{
    version     2.0;
    format      ascii;
    class       dictionary;
    location    "system";
    object      fvSolution;
```

```
}
// * * * * * * * * * * * * * * * * * * * * * * * * * * * * * * * * * * * * * * * * * * * * //

solvers
{
    "rho.*"
    {
        solver          PCG;
        preconditioner  DIC;
        tolerance       0;
        relTol          0;
    }

    p_rgh
    {
        solver          PCG;
        preconditioner  DIC;
        tolerance       1e-8;
        relTol          0.01;
    }

    p_rghFinal
    {
        $p_rgh;
        relTol          0;
    }

    "(U|h|e|k|epsilon|R)"
    {
        solver          PBiCG;
        preconditioner  DILU;
        tolerance       1e-6;
        relTol          0.1;
    }

    "(U|h|e|k|epsilon|R)Final"
    {
        $U;
        relTol          0;
    }
}
```

```
PIMPLE
{
    momentumPredictor yes;
    nOuterCorrectors 1;
    nCorrectors     2;
    nNonOrthogonalCorrectors 0;
    pRefPoint (0 0 0);
    pRefValue 0;
}
```